Scheme for the excitation of thorium-229 nuclei based on electronic bridge excitation*

Lin Li (https://orcid.org/0000-0001-9177-7867),[1,2] Zi Li,[1,2] Chen Wang,[1,2] Wen-Ting Gan,[1,2] Xia Hua,[1,†] and Xin Tong[1,‡]

[1]*State Key Laboratory of Magnetic Resonance and Atomic and Molecular Physics, Innovation Academy for Precision Measurement Science and Technology, Chinese Academy of Sciences, Wuhan 430071, China*

[2]*University of Chinese Academy of Sciences, Beijing 100049, China*

Thorium-229 possesses the lowest first nuclear excited state, with an energy of approximately 8 eV. The extremely narrow linewidth of the first nuclear excited state, with an uncertainty of 53 THz, prevents direct laser excitation and realization of the nuclear clock. We present a proposal using the Coulomb crystal of a linear chain formed by $^{229}Th^{3+}$ ions, where the nuclei of $^{229}Th^{3+}$ ions in the ion trap are excited by the electronic bridge (EB) process. The $7P_{1/2}$ state of the thorium-229 nuclear ground state is chosen for EB excitation. Using the two-level optical Bloch equation under experimental conditions, we calculate that two out of 36 prepared thorium ions in the Coulomb crystal can be excited to the first nuclear excited state, and it takes approximately 2 h to scan over an uncertainty of 0.22 eV. Taking advantage of the transition enhancement of EB and the long stability of the Coulomb crystal, the energy uncertainty of the first excited state can be limited to the order of 1 GHz.

Keywords: Coulomb crystal, thorium-229, electronic bridge transition, isomeric state

I. INTRODUCTION

The excitation energy between the nuclear ground state and the first nuclear excited state (isomeric state) of thorium-229 (Th-229) is approximately 8 eV [1–4]. The optical transition linewidth of the first nuclear excited state is 10^{-4} Hz [5, 6]. The low isomeric energy and narrow linewidth provide the potential for a resonator with a quality of a factor of 10^{19} and make Th-229 the most suitable choice for the development of nuclear optical clocks [6–8]. Such a Th-229 nuclear clock is expected to be a sensitive probe for the time variation of the fundamental constants of nature and will open opportunities for highly sensitive tests of the fundamental principles of physics, particularly in searches for violations of Einstein's equivalence principle and new particles [9–11].

The isomeric energy is currently measured in two ways: 1) Measuring the kinetic energy of internal conversion electrons from the Th-229 isomeric state. For example, an electron spectrometer has been used to detect the internal conversion electron energy, and the isomeric energy was obtained as 8.28 ± 0.17 eV [4]. 2) Observing the γ radiation from Th-229 excited nuclei. An isomeric energy of 7.8 ± 0.5 eV was obtained using a magnetic microcalorimeter [2]. Subsequently, a 29.2-keV inter-band excitation of the Th-229 nuclear state was observed using synchrotron radiation [3]. Combined with the in-band 29.2-keV transition observed via nuclear rotational spectroscopy, the Th-229 isomeric state energy was determined to be 8.30 ± 0.92 eV [12]. Recently, a more precise magnetic microcalorimeter with improved energy resolution was developed, and an isomeric energy of 8.10 ± 0.17 eV was obtained [1]. Taking different weights for these measurements, the average value of the isomeric state was determined as 8.12 ± 0.11 eV [13]. Its uncertainty corresponds to 53 THz, which is at least 16 orders of magnitude higher than the narrow linewidth of 10^{-4} Hz.

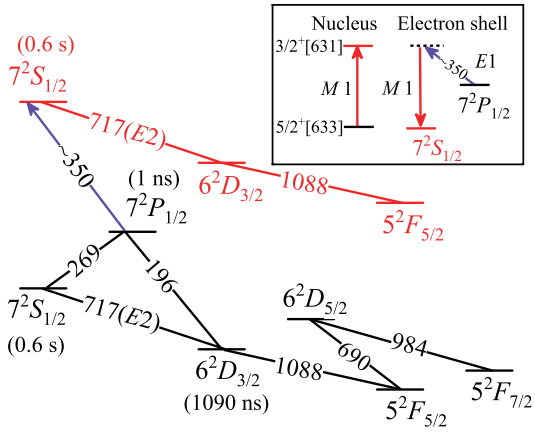

Fig. 1. Diagram of electronic energy levels and electric-dipole transitions of Th-229 triply charged ions. The insert shows the processes of EB excitation, where the red arrows are the 150-nm $M1$ transition. The black horizontal lines indicate the nuclear ground state of Th-229, and the red horizontal lines indicate the isomeric state of Th-229. The purple arrow is the 350-nm EB excitation. The lifetime of the electronic excited state is indicated in the parentheses. The optical transition wavelengths are in nm, and the integers near the atomic levels indicate the principal quantum numbers.

To improve the precision of the isomeric energy, synchrotron radiation has been used to irradiate Th-229 doped in a vacuum ultraviolet (VUV) transparent crystal, and γ photons were detected from the decay of the Th-229 excited nuclei. This measurement excluded approximately half of the favored transition search area [14]. Another scheme was proposed to achieve Th-229 nuclei excitation via electron capture and detect the isomeric state of ions in heavy-ion storage rings [15]. Recently, an optical frequency comb was proposed to irradiate a Th-229 dioxide film, and the isomeric energy was measured based on the internal conversion process [16]. Furthermore, a new approach has been suggested to excite the

* This work was supported by the National Natural Science Foundation of China (No. 11804372).

† huaxia@wipm.ac.cn

‡ tongxin@wipm.ac.cn

isomeric Th-229 nuclear state via laser-driven electron recollision. The advantage of this approach is that it does not require precise knowledge of the isomeric energy [17].

In this paper, we propose the excitation of the nuclei of $^{229}Th^{3+}$ ions in the ion trap via electronic bridge (EB) excitation and compare it with direct nuclear excitation via a pulsed laser. As shown in the inset of Fig. 1, EB excitation starts from an electric dipole ($E1$) transition, which is utilized to excite the electrons from an initial state to a virtual intermediate state. Subsequently, the intermediate state decays via the magnetic dipole ($M1$) transition, and the nuclear ground state $5/2^+[633]$ is excited to the isomeric state $3/2^+[631]$ simultaneously. To date, EB schemes for nuclear excitation have been theoretically investigated for $^{229g}Th^{+}$ [18], $^{229}Th^{2+}$ [19], $^{229}Th^{3+}$ [20–22], and $^{229}Th^{35+}$ [23]. Our proposed experiment is based on EB excitation in triply charged $^{229}Th^{3+}$ ions. Owing to their simple electronic energy levels, the trapped $^{229}Th^{3+}$ ions can be laser-cooled to form a linear-chain Coulomb crystal using two closed transitions in the nuclear ground state of $^{229}Th^{3+}$ ($^{229g}Th^{3+}$) [24]. When the $^{229g}Th^{3+}$ ions are prepared in the $7P_{1/2}$ state, EB excitation is triggered by a 350-nm laser, and isomeric states are expected to be populated. Finally, the isomeric state is detected based on the isomer shift of the cooling lasers [7].

II. PREPARATION OF $^{229g}Th^{3+}$ ION COULOMB CRYSTALS AND THE $7P_{1/2}$ STATE

$^{229g}Th^{3+}$ ions are typically produced by laser ablation [24, 25]. The linear Paul trap used to trap $^{229g}Th^{3+}$ ions are described in detail in our previous papers [26, 27]. The trapped $^{229g}Th^{3+}$ ions are laser-cooled to form a Coulomb crystal.

The energy levels of laser cooling and fluorescence detection of the trapped ions are shown in Fig. 2. The $^{229g}Th^{3+}$ ions are Doppler-laser-cooled on a $5^2F_{5/2} \leftrightarrow 6^2D_{3/2}$ transition at 1088 nm. Alternatively, a closed optical transition of the three-level Λ system, $5^2F_{5/2} \leftrightarrow 6^2D_{5/2} \leftrightarrow 5^2F_{7/2}$, can be used to laser-cool the $^{229g}Th^{3+}$ ions with two lasers at 690 nm and 984 nm [7]. The population in the three hyperfine levels of $|\,5F_{5/2}, F = 3, 4, 5\rangle$ can be transferred to $|\,5F_{5/2}, F = 1\rangle$ and $|\,5F_{5/2}, F = 2\rangle$ via the $6^2D_{3/2}$ state, and the population in the $|\,5F_{7/2}, F = 1\rangle$ state is cumulated as shown in Fig. 2. Therefore, the ions at other hyperfine levels are transferred to the closed system of $5^2F_{5/2} \leftrightarrow 6^2D_{5/2} \leftrightarrow 5^2F_{7/2}$, and the second laser cooling cycle is realized.

Once the $^{229g}Th^{3+}$ ions are laser-cooled to 50 μK, the Doppler broadening of the transition $6^2D_{5/2} \rightarrow 5^2F_{7/2}$ at 984 nm is approximately 1 MHz [24]. At this temperature, the corresponding Doppler broadenings of direct nuclear excitation at 150 nm and EB excitation at 350 nm are estimated to be 6.5 MHz and 2.8 MHz, respectively. The shapes of Coulomb crystals can be manipulated into a linear chain by adjusting the radiofrequency (RF) and endcap voltages [28]. Two-dimensional and linear-chain Coulomb crystals can be simulated with single-ion resolution [29, 30]. Using the GPU-accelerated LAMMPS [31] wrapped by the LIon package

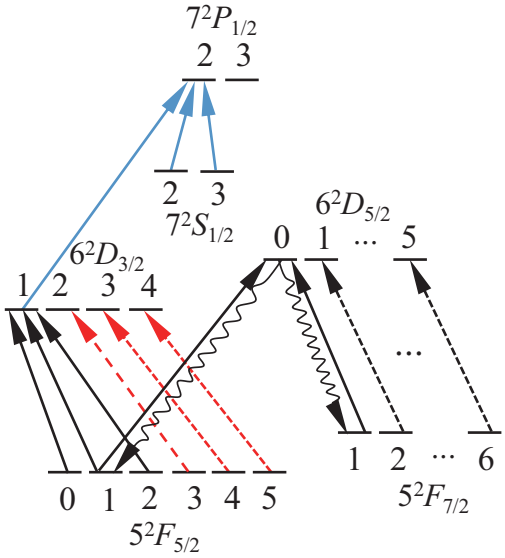

Fig. 2. State preparation scheme of $^{229g}Th^{3+}$ ions. The cooling scheme utilizes the two closed system indicated by the black solid arrows. The wavy arrows indicate spontaneous radiation, and the blue solid arrows indicate the transition to the $7P_{1/2}$ state. The red dashed arrows are the transitions to transfer ions at $|\,5F_{5/2}, F = 3, 4, 5\rangle$ to $|\,5F_{5/2}, F = 1\rangle$ and $|\,5F_{5/2}, F = 2\rangle$. The black dashed arrows are the transitions to transfer ions at $|\,5F_{7/2}, F = 2, 3, 4, 5, 6\rangle$ to $|\,5F_{7/2}, F = 1\rangle$. The integers near the atomic levels indicate the total angular momentum quantum numbers F.

[32], a Coulomb crystal consisting of 36 $^{229g}Th^{3+}$ ions are simulated, as shown in Fig. 3. When an endcap voltage of 0.2 V and an RF voltage (200 V_{0-pk}) of 2 MHz are applied to the ion trap, a linear-chain Coulomb crystal of 36 $^{229g}Th^{3+}$ ions (Fig. 3(c)) is obtained. When an RF voltage (200 V_{0-pk}) of 2 MHz and endcap voltage of 0.025 V are applied to the ion trap, a linear-chain Coulomb crystal of 100 $^{229g}Th^{3+}$ ions is obtained. From the simulation results, the motion amplitude of ions in the x- and y-directions (radial direction) is known to be less than 0.6 μm when the temperature is below 5 mK, which is consistent with the motion amplitude of single ions [33]. Therefore, a strongly focused laser spot size of over 1.2 μm is required to increase the EB and direct nuclear excitation rates.

To induce EB excitation from the $7P_{1/2}$ state of the $^{229g}Th^{3+}$ ions, the three-level transition $5^2F_{5/2} \rightarrow 6^2D_{3/2} \rightarrow 7^2P_{1/2}$ can be used to accumulate the population at the $7P_{1/2}$ state. Once the $^{229g}Th^{3+}$ ions are laser-cooled to 50 μK, the 690-nm and 984-nm lasers are turned off in sequence to maintain the ions at the $5^2F_{5/2}$ state, and the 1088-nm laser is kept on. To transfer a large population to the $7^2P_{1/2}$ state with a lifetime of 1 ns, both the 269-nm and 196-nm transitions are excited simultaneously, as shown in Fig. 1. The natural linewidths of the 269-nm and 196-nm transitions are approximately $2\pi \cdot 32$ MHz and $2\pi \cdot 127$ MHz, respectively [34]. Continuous wave (CW) lasers at both wavelengths are commercially available [35].

The spontaneous radiation rate of the hyperfine structure

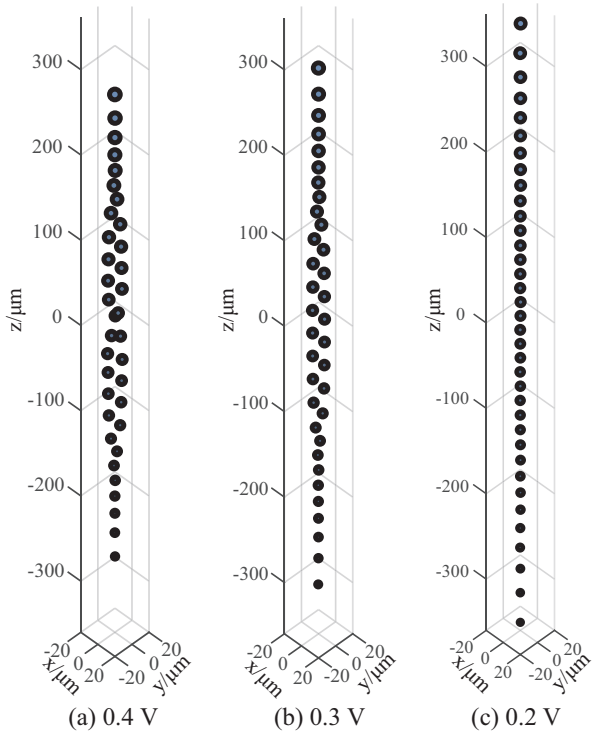

(a) 0.4 V (b) 0.3 V (c) 0.2 V

Fig. 3. Simulation results of a Coulomb crystal consisting of 36 $^{229g}Th^{3+}$ ions. With the same RF voltages (200 V_{0-pk}), the Coulomb crystals' shapes are changed under different endcap voltages (a) 0.4 V, (b) 0.3 V, and (c) 0.2 V. See text for details.

level transitions between two electronic energy levels is [36]

$$\Gamma_{f\to i} = |\langle \xi_f J_f I^g F_f \| d \| \xi_i J_i I^g F_i \rangle|^2 \frac{4\omega^3}{3\hbar c^3}, \tag{1}$$

where ξ_i (ξ_f) incorporates all other electronic quantum numbers, J_i (J_f) is the total electronic quantum number of the initial (final) state, F_i (F_f) is the total quantum number of the initial (final) state, I^g is the nuclear spin of the nuclear ground state, d is the electron dipole, ω is the angular frequency of the electronic transition, $\hbar$ is the reduced Planck constant, and c is the speed of light in a vacuum. $|\langle J_f I^g F_f \| d \| J_i I^g F_i \rangle|^2$ is the transition strength of the hyperfine structure level, which can be expressed as

$$|\langle \xi_f J_f I^g F_f \| d \| \xi_i J_i I^g F_i \rangle|^2 = (2F_i+1)(2F_f+1) \begin{Bmatrix} J_f & F_f & I^g \\ F_i & J_i & 1 \end{Bmatrix}^2 |\langle J_f \| d \| J_i \rangle|^2, \tag{2}$$

where $|\langle J_f \| d \| J_i \rangle|^2$ denotes the transition strength of the electronic energy levels. The spontaneous radiation rate of the electronic energy levels is

$$\Gamma_{spont} = |\langle \xi_f J_f \| d \| \xi_i J_i \rangle|^2 \frac{4\omega^3}{3\hbar c^3}. \tag{3}$$

The excitation rate of the hyperfine structure levels between the two electronic energy levels is [37]

$$\Gamma_{exc} = \Gamma_{f\to i} \frac{\pi^2 c^2}{\hbar\omega^3} P_\omega \frac{2F_f+1}{2F_i+1}, \tag{4}$$

where P_ω denotes the laser spectral intensity. The stimulated emission rate of the hyperfine structure levels between the two electronic energy levels is

$$\Gamma_{sti} = \Gamma_{exc} \frac{2F_i+1}{2F_f+1}. \tag{5}$$

With a laser power of 1 mW and 100-μm laser spot sizes for 1088 nm, 269 nm, and 196 nm lasers, the steady-state condition can be fulfilled for all $5^2F_{5/2}$, $7^2S_{1/2}$, $6^2D_{3/2}$, and $7^2P_{1/2}$ states under continuous illumination. For multiple hyperfine structure transitions between electronic transitions $5^2F_{5/2} \leftrightarrow 6^2D_{3/2}$ and $7^2S_{1/2} \leftrightarrow 7^2P_{1/2}$, the power of the lasers is divided equally. Thus, after state preparation, the population of the $|7P_{1/2}, F=2\rangle$ state accounts for approximately 12% of the total number of trapped ions.

III. CALCULATION OF THE POPULATION IN THE NUCLEAR EXCITED STATE

The time-dependent nuclear excitation probability $\rho_{exc}(t)$ for a single nucleus under resonant irradiation is given by Torrey's solution to the optical Bloch equations as follows [38–40]:

① $\Omega_{eg} > \frac{|\Gamma-\tilde{\Gamma}|}{2}$,

$$\rho_{exc}(t) = \frac{\Omega_{eg}^2}{2(\Gamma\tilde{\Gamma}+\Omega_{eg}^2)} \left[1 - e^{-\frac{1}{2}(\Gamma+\tilde{\Gamma})t} \times \left(\cos(\lambda t) + \frac{\Gamma+\tilde{\Gamma}}{2\lambda}\sin(\lambda t)\right)\right], \tag{6}$$

② $\Omega_{eg} < \frac{|\Gamma-\tilde{\Gamma}|}{2}$,

$$\rho_{exc}(t) = \frac{\Omega_{eg}^2}{2(\Gamma\tilde{\Gamma}+\Omega_{eg}^2)} \left[1 - e^{-\frac{1}{2}(\Gamma+\tilde{\Gamma})t} \times \left(\cosh(\lambda t) + \frac{\Gamma+\tilde{\Gamma}}{2\lambda}\sinh(\lambda t)\right)\right]. \tag{7}$$

Here, Ω_{eg} denotes the Rabi frequency between the isomeric and nuclear ground states. $\Gamma = \Gamma_\gamma + \Gamma_{nr}$ is the total linewidth

of the isomeric state, and Γ_γ denotes the γ decay rate of the isomeric state. Because the ionization energy of $^{229g}Th^{3+}$ (28.6 eV) is considerably greater than the energy of the isomeric state, the internal conversion process is strongly forbidden [41]. The possible non-radiative transition linewidth Γ_{nr} is dominated by the EB transition for $^{229g}Th^{3+}$. $\tilde{\Gamma} = \frac{\Gamma+\Gamma_L}{2} + \Gamma_{add}$ denotes the total transition linewidth [40], Γ_L denotes the laser linewidth used for nuclear excitation, and Γ_{add} is the additional incoherent linewidth, such as phonon coupling of ions in a Coulomb crystal. Because Γ_{add} is significantly smaller than the laser linewidth Γ_L, the influence of the incoherent linewidth is negligible. t denotes the interaction time between the laser and $^{229g}Th^{3+}$ ions. Here, $\lambda = |\Omega_{eg}^2 - (\Gamma - \tilde{\Gamma})^2/4|$.

Under the resonant condition, the Rabi frequency between the isomeric state and nuclear ground state is [39]

$$\Omega_{eg} = \sqrt{\frac{2\pi c^2 I C_{eg}^2 \Gamma}{\hbar \omega_m^3}}. \tag{8}$$

Here, I is the intensity of the excitation laser, and ω_m is the angular frequency of the nuclear transition. The Zeeman splitting caused by the geomagnetic field between the two outermost lines is below 1 kHz and is negligible. Therefore, the Clebsch–Gordan coefficient of the sub-state transition between the isomeric state and the nuclear ground state C_{eg} is 1 [16].

Assuming that the intensities of all lasers have a Gaussian distribution, the Rabi frequency can be modified via the following two situations:

i) If the laser linewidth (Γ_L) is greater than the Doppler-broadening linewidth (Γ_D), only part of the laser with a matching frequency range can effectively interact with the triply charged thorium ions. The equivalent Doppler-broadening linewidth is

$$\Gamma_D^{'} = \frac{1}{2}\sqrt{\frac{\pi}{\ln 2}}\Gamma_D. \tag{9}$$

The effective laser intensity is

$$I_{eff} = I \int_{-\frac{\Gamma_D^{'}}{2}}^{\frac{\Gamma_D^{'}}{2}} g_L(\omega) \mathrm{d}\omega. \tag{10}$$

The modified Rabi frequency is

$$\Omega_{eg}^{'} = \sqrt{\frac{2\pi c^2 I_{eff} C_{eg}^2 \Gamma}{\hbar \omega_m^3}}. \tag{11}$$

ii) If the laser linewidth (Γ_L) is smaller than the Doppler-broadening linewidth (Γ_D), only part of the ions interact with the laser light at the frequency resonance at a certain time, and the equivalent laser linewidth is

$$\Gamma_L^{'} = \frac{1}{2}\sqrt{\frac{\pi}{\ln 2}}\Gamma_L. \tag{12}$$

The effective Doppler-broadening linewidth is

$$\Gamma_{eff} = \Gamma \int_{-\frac{\Gamma_L^{'}}{2}}^{\frac{\Gamma_L^{'}}{2}} g_D(\omega) \mathrm{d}\omega. \tag{13}$$

The modified Rabi frequency is

$$\Omega_{eg}^{'} = \sqrt{\frac{2\pi c^2 I C_{eg}^2 \Gamma_{eff}}{\hbar \omega_m^3}}. \tag{14}$$

IV. DIRECT NUCLEAR EXCITATION

The Th-229 isomeric energy is 8.12 ± 0.11 eV, corresponding to a wavelength of $150.7-154.8$ nm. Currently, available light sources such as the VUV pulsed laser [42], synchrotron radiation light source [14], and the 7th harmonic of a Yb-doped fiber laser [16, 43–45] are suitable candidates for direct nuclear excitation. Here, based on resonance-enhanced four-wave mixing, the parameters of a tunable and pulsed VUV laser source are a pulse energy of E_L = 13.2 µJ around 150 nm, a bandwidth of $\delta\nu_L$ = 15 GHz, and a repetition rate of R_L = 10 Hz, which are used to calculate the direct nuclear excitation rate [42].

Assuming a strongly focused laser with a 3-μm spot radius to irradiate the linear chain of 100 ions, the corresponding laser intensity $I = \frac{E_L R_L}{\pi r^2} = 4.67 \times 10^6$ W/m^2 can be obtained. The temperature of Th^{3+} ions is 50 μK, and the corresponding Doppler-broadening linewidth Γ_D = 6.5 MHz is narrower than the laser linewidth. Therefore, the modified Rabi frequency at resonance $\Omega_{eg}^{'}(\delta = 0)$ = 107 Hz can be obtained based on Eq. (9)−(11), which is significantly smaller than the total transition linewidth $\tilde{\Gamma}$ shown in Table 1. In this case, $\Omega_{eg}^{'} < \frac{|\Gamma-\tilde{\Gamma}|}{2}$ is satisfied. The number of excited nuclei is calculated as a function of time using Eq. (7). As shown in Fig. 4, the number of excited Th-229 nuclei is only 0.12 out of 100 Th-229 ions and reaches saturation at an irradiation time of 30000 s. The required laser irradiation time is beyond the stable trapping time; therefore, no Th-229 isomeric state can be detected under the current experimental conditions.

V. ELECTRONIC BRIDGE EXCITATION

Direct nuclear excitation is limited by the natural linewidth of the isomeric state and the power of the excitation laser. If EB excitation occurs, the transition linewidth can be increased by approximately 40 times compared with direct nuclear excitation [46]. EB excitation can be utilized by exciting the quantum state of the electronic state $7P_{1/2}$ of $^{229g}Th^{3+}$ ($7P_{1/2}$ $5/2^+[633]$) to the electronic state $7S_{1/2}$ of $^{229m}Th^{3+}$ ($7S_{1/2}$ $3/2^+[631]$), as shown in Fig. 1. The prepared $^{229g}Th^{3+}$ Coulomb crystal comprising a linear chain of 36 ions is shown in Fig. 3(c), among which there are four

Table 1. **Values of variables used for the calculation of the number of excited nuclei using Eq. (7).**

Variable	Description	Value	Comment
$\tilde{\Gamma}$	Total transition linewidth	$2\pi\cdot$ 7.5 GHz	Significantly larger than the nuclear transition linewidth
Γ_γ	Radiative linewidth	10^{-4} Hz	Estimated from theory
Γ_D	Doppler-broadening linewidth	6.5 MHz	Doppler broadening of ions from direct nuclear excitation
N	Number of ions	100	Laser-cooled ions
Ω_{eg}	Rabi frequency	1156 Hz	Direct excitation between the isomeric and nuclear ground states
$\Omega'_{eg}(\delta=0)$	Modified Rabi frequency	107 Hz	Modified Rabi frequency at resonance

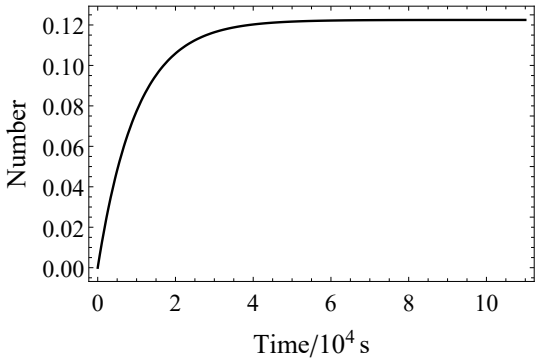

Fig. 4. Expected number of excited nuclei is calculated as a function of time when 100 triply charged Th-229 ions are directly illuminated by a direct excitation laser.

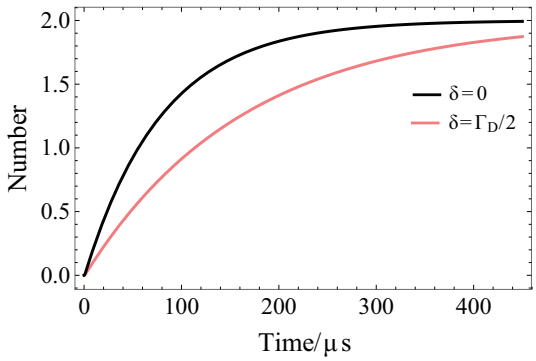

Fig. 5. Expected number of excited nuclei is calculated as a function of time when 36 triply charged Th-229 ions are trapped and four ions are at the $7P_{1/2}$ state.

ions (12% of the total number of trapped ions) in the $7P_{1/2}$ state under steady-state conditions (see Sect. II).

Table 2. Values of variables used for the calculation of the number of excited nuclei using Eq. (7).

Variable	Value	Comment
Γ_L	$2\pi\cdot$ 500 kHz	Larger than the nuclear transition linewidth
Γ_γ	10^{-4} Hz	Estimated from theory
Γ_D	2.8 MHz	Doppler broadening of ions from EB excitation
N	36	Laser-cooled ions
α_{eb}	40	EB decay of Th^{3+} ions
Ω_{eg}	334 kHz	Rabi frequency
$\Omega'_{eg}(\delta=0)$	140 kHz	Modified Ω_{eg} at resonance
$\Omega'_{eg}(\delta=\frac{\Gamma_D}{2})$	98 kHz	Modified Ω_{eg} detune $\frac{\Gamma_D}{2}$

The wavelength of the laser used for EB excitation is 350 nm. A 350-nm laser with a power of 250 mW can be obtained from Toptica DLC TA-SHG pro and focused to a spot size of 10 μm. Thus, an intensity of 7.95×10^8 Wm^{-2} can be achieved. Therefore, the Rabi frequency is estimated as 334 kHz.

The EB laser linewidth, typically 500 kHz at 350 nm, is narrower than the Doppler broadening of the trapped thorium ions. The modified Rabi frequency Ω'_{eg} is 140 kHz at resonance and 98 kHz upon the detuning $\Gamma_D/2$ (shown in Table 2). Then, the condition $\Omega'_{eg} < \frac{|\Gamma-\tilde{\Gamma}|}{2}$ is satisfied, and thus the number of excited nuclei as a function of time can be obtained based on Eq. (7), as shown in Fig. 5. If the excitation energy from the $7P_{1/2}$ state of $^{229g}Th^{3+}$ to the $7S_{1/2}$ state of $^{229m}Th^{3+}$ is at resonance, approximately 2 $^{229g}Th^{3+}$ ions can be excited to the isomeric state after 300-μs irradiation by the 350-nm laser. If the excitation laser is detuned by $\Gamma_D/2$, approximately 1.8 $^{229g}Th^{3+}$ ions can be excited to the isomeric state within the same irradiation time.

After successful EB excitation, Th-229 ions in the isomeric state can be identified based on the different hyperfine structures of the isomeric and nuclear ground states. Detailed hyperfine structures of the isomeric state are shown in Appendix B. After EB nuclear excitation, the EB laser at 350 nm and the state-preparation lasers at 196 nm and 269 nm are all turned off, and the cooling lasers at 690 nm and 984 nm are immediately switched back on and combined with the 1088-nm laser to cool the ions. The nuclear-excited ions remain in the isomeric states and accumulate in the electronic state of $5^2F_{5/2}$, as illustrated in Fig. 1. The remaining nuclear-unexcited ions remain in the nuclear ground state of the Doppler cooling cycle of $5^2F_{5/2}$, $6^2D_{5/2}$, $5^2F_{7/2}$ and $6^2D_{3/2}$. The isomer shifts of the $6D_{5/2}$ and $6D_{3/2}$ electronic states are both approximately 400 MHz [24, 47]. The 690-nm and 984-nm lasers are off-resonance for the Doppler cooling of ions in the isomeric state. As a result, the nuclear-excited $^{229m}Th^{3+}$ ions leave the 690-nm and 984-nm lasers' cooling cycle and appear as dark ions in the Coulomb crystal [7]. In the linear-chain $^{229}Th^{3+}$ ion Coulomb crystal, single ions are distinguishable, and any dark $^{229m}Th^{3+}$ ions generated by a successful EB excitation

event can be detected.

Table 3. Main parameters for 350-nm irradiation on 36 trapped ions.

Variable	Value
Time per scan step	$\approx 300\,\mu s$
Number of ions at the $7P_{1/2}$ state	4
Number of laser-cooled ions	≈ 36
Number of isomeric states per scan step	$2(\delta = 0)$
Number of isomeric states per scan step	$1.8(\delta = \frac{\Gamma_D}{2})$
Time required to scan 0.22 eV	≈ 5670 s

The current reported uncertainty on the isomeric state energy is 0.22 eV [13]. To cover this uncertainty range, approximately 1.9×10^7 scans are required for each scanning interval of the Doppler-broadening linewidth Γ_D. The time required for a single scan step is approximately 300 µs; therefore, the total scan time is approximately 5670 s, as shown in Table 3. The final isomeric energy is determined by the sum of the energy intervals between the electronic state $7P_{1/2}$ of $^{229g}Th^{3+}$ and the electronic state $7S_{1/2}$ of $^{229m}Th^{3+}$ and the photon energy of the 350-nm laser. Because the uncertainty on the natural linewidth of the $7P_{1/2}$ state of $^{229g}Th^{3+}$ is 1 GHz, which is significantly larger than the laser and Doppler-broadening linewidths, the uncertainty on the isomeric energy is of the order of 1 GHz (corresponding to 4×10^{-6} eV), dominated by the natural linewidth of the $7P_{1/2}$ state.

VI. CONCLUSION

In this paper, considering the Doppler broadening of thorium ions in the ion trap, we show that 2 $^{229g}Th^{3+}$ ions out of 36 trapped ions can be excited to the isomeric state under resonant conditions via EB excitation. We propose that a total measurement time of approximately 2 h can be achieved for the current uncertainty on the isomeric state energy of 0.22 eV. If a cryogenic linear Paul trap is used, the ions can be stably trapped for a longer period and the radiative lifetime of the isomeric state can be measured. The utilization of EB excitation can reduce the uncertainty on the Th-229 isomeric energy to approximately 1 GHz. The calculation is based on the theoretical prediction that the transition linewidth of EB excitation is 40 times larger than that of direct nuclear excitation. If EB excitation is not observed, as proposed in this paper, it may indicate that the coupling between the electrons and the nuclear core is not as strong as expected or that the explored nuclear transition energy range is not accurate, and the laser energy used for the EB excitation needs to be increased. However, the successful observation of EB excitation will further improve the accuracy of isomeric energy, pave the way for the development of a nuclear optical clock, test the temporal variation of fundamental constants, and provide new methods for studying nuclear physics.

APPENDIX A. EXPERIMENTAL STEPS

As shown in Fig. 6, the experiments are divided into three steps.

① Laser cooling: The 1088-nm, 984-nm, and 690 nm lasers are turned on to laser-cool the ions into a Coulomb crystal of a linear chain. Later, the 690-nm and 984-nm lasers are turned off in sequence to keep the entire population at the $5F_{5/2}$ state.

② State preparation and nuclear excitation: Once the 690-nm laser is turned off, the 269-nm and 196-nm lasers are turned on to prepare the $^{229g}Th^{3+}$ ions at the $7P_{1/2}$ state, and the 350-nm laser is turned on to excite the Th-229 nuclei from the nuclear ground state to the isomeric state.

③ Detection of the isomeric state: The 350-nm laser is turned off to prohibit the EB transition from $7S_{1/2}$ of the isomeric state and maintain the population of the isomeric state. Simultaneously, the 196-nm and 269-nm lasers are turned off in sequence to cumulate the ions at the four lowest electronic states. Then, the 690-nm and 984-nm lasers are turned on to detect the isomeric state based on the isomer shift.

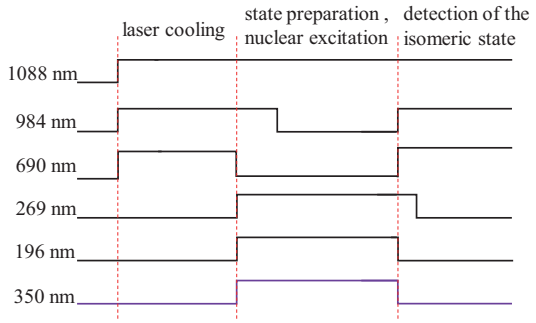

Fig. 6. Experimental steps and the time of each laser switch.

APPENDIX B. HYPERFINE STRUCTURES OF $^{229}Th^{3+}$

The hyperfine structures of $^{229g}Th^{3+}$ are measured as described in [48], where $\mu^g = 0.360(7)\mu_N$, and $Q^g = 3.11(16)$eb. Subsequently, the hyperfine structures of $^{229g}Th^{2+}$ and $^{229m}Th^{2+}$ are measured as described in [47], where $\mu^m = -0.37(6)\mu_N$, and $Q^m = 1.74(6)$eb.

The magnetic dipole (A^m) hyperfine coefficients of $^{229m}Th^{3+}$ are determined using

$$A^m = \frac{A^g I^g \mu^m}{\mu_g I^m}. \tag{B15}$$

The electric quadrupole (B^m) hyperfine coefficients of $^{229m}Th^{3+}$ are determined using

$$B^m = \frac{B^g Q^m}{Q^g}. \tag{B16}$$

The magnetic dipole and electric quadrupole hyperfine coefficients of the four lowest levels of $^{229m}Th^{3+}$ are calculated, as shown in Table 4.

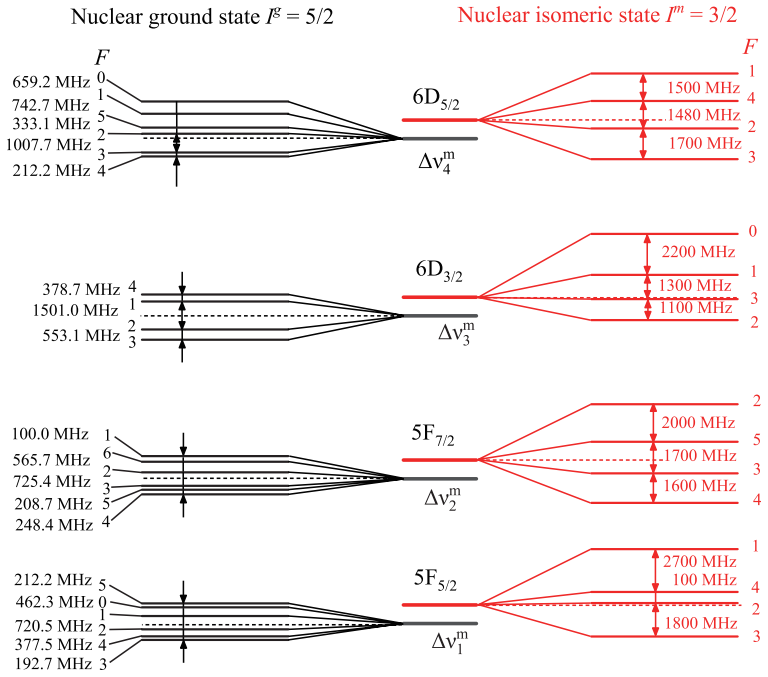

Fig. 7. Four lowest-lying fine structure levels of $^{229}Th^{3+}$, including hyperfine structures. The integers near the atomic levels indicate the total angular momentum quantum numbers F.

Table 4. Magnetic dipole and electric quadrupole hyperfine coefficients of the four lowest levels of $^{229m}Th^{3+}$.

Valence orbital	A^m(MHz)	B^m(MHz)
$5F_{5/2}$	−140(20)	1270(80)
$5F_{7/2}$	−54(9)	1430(90)
$6D_{3/2}$	−270(40)	1270(80)
$6D_{5/2}$	22(4)	1510(90)

Therefore, the hyperfine structures of $^{229m}Th^{3+}$ can be obtained as follows:

$$E_{\rm HFS}(J, I^m, F) = \frac{A^m K}{2} + \frac{B^m[\frac{3}{4}K(K+1) - I^m(I^m+1)J(J+1)]}{2I^m(2I^m-1)(2J-1)}, \quad \text{(B17)}$$

where $K = F(F+1) - J(J+1) - I^m(I^m+1)$.

Using Eq. B17, the hyperfine structures of the four lowest levels of $^{229m}Th^{3+}$ are calculated, as listed in Table. 5

The isomer shift is determined using

$$\Delta\nu^m = F^{'}\delta\langle r^2\rangle, \quad \text{(B18)}$$

where the difference between the mean-square radii of the isomeric and ground states in ^{229}Th is $\delta\langle r^2\rangle$ = 0.012(2)fm^2 [49], and the field shift constant $F^{'}$ can be obtained as shown in Ref. [42]. Therefore, the centers of the hyperfine structures of $^{229m}Th^{3+}$ can be obtained as shown in Table 6.

The hyperfine structures of $^{229m}Th^{3+}$ and $^{229g}Th^{3+}$ are shown in Fig. 7, and $\Delta\nu_i^m$ indicates the isomer shift.

The transition frequency of $|5F_{5/2}, F = 1\rangle \rightarrow |6D_{5/2}, F = 0\rangle$ in $^{229g}Th^{3+}$ is 434282480(32) MHz. The

Table 5. Hyperfine structures of the four lowest levels of $^{229m}Th^{3+}$ (MHz).

Valence orbital	F^m	$^{229m}Th^{3+}$
$5F_{5/2}$	1	3000(200)
	2	140(70)
	3	−1700(100)
	4	270(90)
$5F_{7/2}$	2	3000(200)
	3	−690(70)
	4	−2300(100)
	5	970(90)
$6D_{3/2}$	0	3400(200)
	1	1200(100)
	2	−1230(90)
	3	−130(90)
$6D_{5/2}$	1	2500(200)
	2	−450(30)
	3	−2100(100)
	4	1030(60)

Table 6. Centers of the hyperfine structures of the four lowest levels of $^{229}Th^{3+}$ (MHz).

Valence orbital	$^{229g}Th^{3+}$	$^{229m}Th^{3+}$
$5F_{5/2}$	0	0
$5F_{7/2}$	129671430(40)	129671450(50)
$6D_{3/2}$	275596727(31)	275597100(100)
$6D_{5/2}$	434280888(31)	434281300(100)

hyperfine transitions between the $5F_{5/2}$ and $6D_{5/2}$ states of $^{229m}Th^{3+}$ are listed in Table 7.

The transition frequency of $|5F_{5/2}, F = 3\rangle \rightarrow |6D_{5/2}, F = 2\rangle$ in $^{229m}Th^{3+}$ is close to that of $|5F_{5/2}, F = 1\rangle$

Table 7. Hyperfine transitions from the $5F_{5/2}$ state to the $6D_{5/2}$ state of $^{229m}Th^{3+}$ (MHz).

Transition		Transition	
$1 \rightarrow 1$	434280800(300)	$2 \rightarrow 1$	434283700(200)
$1 \rightarrow 2$	434277900(200)	$2 \rightarrow 2$	434280700(100)
$3 \rightarrow 2$	434282600(100)	$2 \rightarrow 3$	434279100(200)
$3 \rightarrow 3$	434280900(200)		
$3 \rightarrow 4$	434284000(200)		

$\rightarrow |\, 6D_{5/2}, F = 0\rangle$ in $^{229g}Th^{3+}$.

The transition frequency of $|\, 5D_{5/2}, F = 0\rangle \rightarrow |\, 5F_{7/2}, F = 1\rangle$ in $^{229g}Th^{3+}$ is 304610430(34) MHz. The hyperfine transitions between the $|6D_{5/2}, F = 2\rangle$ and $5F_{7/2}$ states of $^{229m}Th^{3+}$ are listed in Table 8. As a result, the 690-nm and 984-nm lasers used to cool the $^{229g}Th^{3+}$ ions cannot form the closed optical cycle required for the laser-cooling of $^{229m}Th^{3+}$ ions.

Table 8. Hyperfine transitions between the $|6D_{5/2}, F = 2\rangle$ and $5F_{7/2}$ states of $^{229m}Th^{3+}$ (MHz).

Transition	
$2 \rightarrow 2$	304606900 (200)
$2 \rightarrow 3$	304610500 (100)

[1] S. Tomas, G. Jeschua, H. Daniel *et al.*, Measurement of the Th-229 isomer energy with a magnetic microcalorimeter. Phys. Rev. Lett. **125**, 142503 (2020). doi: 10.1103/PhysRevLett.125.142503

[2] B. R. Beck, J. A. Becker, P. Beiersdorfer *et al.*, Energy splitting of the ground-state doublet in the nucleus ^{229}Th. Phys. Rev. Lett. **98**, 142501 (2007). DOI: 10.1103/PhysRevLett.98.142501

[3] A. Yamaguchi, H. Muramatsu, T. Hayas *et al.*, Energy of the ^{229}Th nuclear clock isomer determined by absolute gamma-ray energy difference. Phys. Rev. Lett. **123**, 222501 (2019). DOI: 10.1038/s41586-019-1533-4

[4] B. Seiferle, L. von der Wense, P. V. Bilous *et al.*, Energy of the ^{229}Th nuclear clock transition. Nature **573**, 243-246 (2019). DOI: 10.1038/s41586-019-1533-4

[5] N. Minkov and A. Palffy, Theoretical predictions for the magnetic dipole moment of ^{229m}Th. Phys. Rev. Lett. **122**, 162502 (2019). DOI: 10.1103/PhysRevLett.122.162502

[6] L. von der Wense, B. Seiferle, The ^{229}Th isomer: prospects for a nuclear optical clock. Eur. Phys. J. A **56**, 277 (2020). DOI: 10.1140/epja/s10050-020-00263-0

[7] E. Peik and Chr.Tamm, Nuclear laser spectroscopy of the 3.5 eV transition in Th-229. EPL **61**, 181 (2003). DOI: 10.1209/epl/i2003-00210-x

[8] C. J. Campbell, A. G. Radnaev, A. Kuzmich *et al.*, Single-ion nuclear clock for metrology at the 19th decimal place. Phys. Rev. Lett. **108**, 120802 (2012). DOI: 10.1103/PhysRevLett.108.120802

[9] V.V. Flambaum, Enhanced effect of temporal variation of the fine structure constant and the strong interaction in ^{229}Th. Phys. Rev. Lett. **97**, 092502 (2006). DOI: 10.1103/PhysRevLett.97.092502

[10] E. Peik, T. Schumm, M. Safronova *et al.*, Nuclear clocks for testing fundamental physics. Quantum Sci. Technol. **6**, 034002 (2021). DOI: 10.1088/2058-9565/abe9c2

[11] P. Fadeev, J. Berengut, V. Flambaum, Sensitivity of Th-229 nuclear clock transition to variation of the fine-structure constant. Phys. Rev. A **102**, 052833 (2020). DOI: 10.1103/PhysRevA.102.052833

[12] T. Masuda, A. Yoshimi, A. Fujieda *et al.*, X-ray pumping of the ^{229}Th nuclear clock isomer. Nature **573**, 238–242 (2019). DOI: 10.1038/s41586-019-1542-3

[13] L. von der Wense, Ticking toward a nuclear clock. Physics **13**, 152 (2020). DOI: 10.1103/Physics.13.152

[14] J. Jeet, C. Schneider, S. T. Sullivan *et al.*, Results of a direct search using synchrotron radiation for the low-energy ^{229}Th nuclear isomeric transition. Phys. Rev. Lett. **114**, 253001 (2015). DOI: 10.1103/PhysRevLett.114.253001

[15] X. Ma, W. Wen, Z. Huang *et al.*, Proposal for precision determination of 7.8 eV isomeric state in ^{229}Th at heavy ion storage ring. Phys. Scr. **2015**, 014012 (2015). DOI: 10.1088/0031-8949/2015/T166/014012

[16] L. von der Wense, C.K. Zhang, Concepts for direct frequency-comb spectroscopy of ^{229m}Th and an internal-conversion-based solid-state nuclear clock. Eur. Phys. J. D **74**, 146 (2020). DOI: 10.1140/epjd/e2020-100582-5

[17] W. Wang, J. Zhou, B.Q. Liu *et al.*, Exciting the Isomeric ^{229}Th Nuclear State via Laser-Driven Electron Recollision. Phys. Rev. Lett. **127**, 052501 (2021). DOI: 10.1103/PhysRevLett.127.052501

[18] S.G. Porsev, V.V. Flambaum, Electronic bridge process in ^{229}Th^{+}. Phys. Rev. A **81**, 042516 (2010). DOI: 10.1103/PhysRevA.81.042516

[19] E. Peik, M. Okhapkin, Nuclear clocks based on resonant excitation of γ-transitions. CR. Phys. **16**, 516-523 (2015). DOI: 10.1016/j.crhy.2015.02.007

[20] S.G. Porsev, V.V. Flambaum, Effect of atomic electrons on the 7.6-eV nuclear transition in ^{229}Th^{3+}. Phys. Rev. A **81**, 032504 (2010). DOI: 10.1103/PhysRevA.81.032504

[21] P.V. Bilous, E. Peik, A. Pálffy, Laser-induced electronic bridge for characterization of the ^{229m}Th $\rightarrow$ ^{229g}Th nuclear transition with a tunable optical laser. New J Phys. **20**, 013016 (2018). DOI: 10.1088/1367-2630/aa9cd9

[22] N.Q. Cai, G.Q. Zhang, C.B. Fu *et al.*, Populating ^{229m}Th via two-photon electronic bridge mechanism. Nucl. Sci. Tech. **32**, 59 (2021). DOI: 10.1007/s41365-021-00900-3

[23] P.V. Bilous, H. Bekker, J.C. Berengut *et al.*, Electronic bridge excitation in highly charged ^{229}Th ions. Phys. Rev. Lett. **124**, 192502 (2020). DOI: 10.1103/PhysRevLett.124.192502

[24] C.J. Campbell, A.G. Radnaev, A. Kuzmich, Wigner crystals of ^{229}Th for optical excitation of the nuclear isomer. Phys. Rev. Lett. **106**, 223001 (2011). DOI: 10.1103/PhysRevLett.106.223001

[25] C.J. Campbell, A.V. Steele, L.R. Churchill *et al.*, Multiply charged thorium crystals for nuclear laser spectroscopy. Phys. Rev. Lett. **102**, 233004 (2009). DOI: 10.1103/PhysRevLett.102.233004

[26] H.X. Li, Y. Zhang, S.G. He *et al.*, Determination of the geo-

metric parameters κ_z and κ_r of a linear Paul trap. Chinese J Phys. **60**, 61-67 (2019). DOI: 10.1016/j.cjph.2019.03.017

[27] M. Li, Y. Zhang, Q.Y. Zhang *et al*., An efficient method for producing $^9Be^+$ ions using a 2+ 1 resonance-enhanced multi-photon ionization process. J. Phys. B At. Mol. Opt. Phys. **55**, 035002 (2022). DOI: 10.1088/1361-6455/ac4c8f

[28] H. C. Nägerl, W. Bechter, J. Eschner *et al*., Ion strings for quantum gates. Appl. Phys. B **66**, 603–608 (1998). DOI: 10.1007/s003400050443

[29] K. Okada, M. Wada, T. Takayanagi *et al*., Characterization of ion Coulomb crystals in a linear Paul trap. Phys. Rev. A **81**, 013420 (2010). DOI: 10.1103/PhysRevA.81.013420

[30] M.T. Bell, A.D. Gingell, J.M. Oldham *et al*., Ion-molecule chemistry at very low temperatures: cold chemical reactions between Coulomb-crystallized ions and velocity-selected neutral molecules. Faraday Discuss. **142**, 73-91 (2009). DOI: 10.1039/b818733a

[31] S. Plimpton, Fast parallel algorithms for short-range molecular dynamics. J. Comput. Phys. **117**, 1–19 (1995). DOI: 10.1006/jcph.1995.1039

[32] E. Bentine, C. J. Foot, D. Trypogeorgos, (py)LIon: A package for simulating trapped ion trajectories. Comput. Phys. Commun. **253**, 107187 (2020). DOI: 10.1016/j.cpc.2020.107187

[33] P. Richerme, Two-dimensional ion crystals in radio-frequency traps for quantum simulation. Phys. Rev. A **94**, 032320 (2016). DOI: 10.1103/PhysRevA.94.032320

[34] U.I. Safronova, W.R. Johnson, M.S. Safronova, Excitation energies, polarizabilities, multipole transition rates, and lifetimes in ThIV. Phys. Rev. A **76**, 042504 (2007). DOI: 10.1103/PhysRevA.76.042504

[35] L. Kang, Z. Lin, Deep-ultraviolet nonlinear optical crystals: concept development and materials discovery. Sci. Appl. **11**, 201 (2022). DOI: 10.1038/s41377-022-00899-1

[36] M. Auzinsh, D. Budker, S. Rochester, *Optically polarized atoms: understanding light-atom interactions*. 1nd edn. (Oxford, New York, 2010), pp. 141–144

[37] I. I. Sobelman, *Atomic spectra and radiative transitions* . 2nd edn. (Springer Berlin, Heidelberg, 1992), pp. 203–204

[38] H. C. Torrey, Transient nutations in nuclear magnetic resonance. Phys. Rev. **76**, 1059 (1949). DOI: 10.1103/PhysRev.76.1059

[39] P. J. Colmenares, J. L. Paz, On the analytical solution of the optical Bloch equations. Opt. Commun. **284**, 5171–5176 (2011). DOI: 10.1016/j.optcom.2011.07.008

[40] L. von der Wense, B. Seiferle, P. V. Bilous *et al*., The theory of direct laser excitation of nuclear transitions. Eur. Phys. J. A **56**: 176 (2020). DOI: 10.1140/epja/s10050-020-00177-x

[41] P.F.A. Klinkenberg, Spectral structure of trebly ionized thorium, Th IV. Physica. B+C **151**, 552-567 (1988). DOI: 10.1016/0378-4363(88)90312-9

[42] S. J. Hanna, P. Campuzano-Jost, E. A. Simpson *et al*., A new broadly tunable (7.4−10.2eV) laser based VUV light source and its first application to aerosol mass spectrometry. Int. J. Mass Spectrom. **279**, 134-146 (2009). DOI: 10.1016/j.ijms.2022.116952

[43] C. Zhang, S.B. Schoun, C.M. Heyl *et al*., Noncollinear enhancement cavity for record-high out-coupling efficiency of an extreme-UV frequency comb. Phys. Rev. Lett. **125**, 093902 (2020). DOI: 10.1103/PhysRevLett.125.093902

[44] A. Cingoz, D.C. Yost, T.K. Allison *et al*., Direct frequency comb spectroscopy in the extreme ultraviolet. Nature **482**, 68–71 (2012). DOI: 10.1038/nature10711

[45] I. Pupeza, S. Holzberger, T. Eidam *et al*., Compact high-repetition-rate source of coherent 100 eV radiation. Nat. Photon. **7**, 608–612 (2013). DOI: 10.1038/nphoton.2013.156

[46] R. A. Müller, A. V. Volotka, S. Fritzsche *et al*., Theoretical analysis of the electron bridge process in $^{229}Th^{3+}$. Nucl. Instrum. Meth. B **408**, 84–88 (2017). DOI: 10.1016/j.nimb.2017.05.004

[47] J. Thielking, M. V. Okhapkin, P. Głowacki *et al*., Laser spectroscopic characterization of the nuclear-clock isomer ^{229m}Th. Nature **556**, 321–325 (2018). DOI: 10.1038/s41586-018-0011-8

[48] M. S. Safronova, U. I. Safronova, A. G. RadnaeM *et al*., Magnetic dipole and electric quadrupole moments of the ^{229}Th nucleus. Phys. Rev. A **88**, 060501(R) (2013). DOI: 10.1103/PhysRevA.88.060501

[49] J.C. Berengut, V. A. Dzuba, V.V. Flambaum *et al*., Proposed Experimental Method to Determine α Sensitivity of Splitting between Ground and 7.6 eV Isomeric States in ^{229}Th. Phys. Rev. Lett. **102**, 210801 (2009). DOI: 10.1103/PhysRevLett.102.210801